

Reactions between CH_4^+ and $\text{C}_2\text{H}_5\text{OH}$

A.Y. Kok, P.A. Zeijlmans van Emmichoven*, A. Niehaus

Debye Institute, Utrecht University, Princetonplein 5, 3584 CC Utrecht, The Netherlands

Received 11 December 2001; accepted 4 March 2002

Abstract

We report results of an experimental investigation of the reactions of CH_4^+ ions colliding at selected relative kinetic energies in the eV region with $\text{C}_2\text{H}_5\text{OH}$ molecules. Employing the “photo-electron product ion coincidence method (PEPICO),” also the internal energy of the CH_4^+ ion is controlled and varied between 0 and 1.7 eV. It is found that the product ions are formed in two steps, where the first step is either a proton transfer leading to $\text{C}_2\text{H}_5\text{OHH}^+$, or an electron transfer leading to $\text{C}_2\text{H}_5\text{OH}^+$. No indication for the occurrence of rearrangement or association processes is found. The ions formed in the first direct reaction step are found to dissociate partly, leading to a final product ion mass spectrum consisting of the six masses, 47, 46, 45, 31, 29, 19 corresponding to the ions $\text{C}_2\text{H}_5\text{OHH}^+$, $\text{C}_2\text{H}_5\text{OH}^+$, $\text{C}_2\text{H}_5\text{O}^+$, CH_2OH^+ , C_2H_5^+ , and H_3O^+ , respectively. The distribution of the abundances of these masses is found not to change significantly when the average relative kinetic energy is varied between 0.2 and 6 eV, and the internal energy of CH_4^+ is varied between 0 and 1.7 eV. (Int J Mass Spectrom 223–224 (2003) 81–89) © 2002 Elsevier Science B.V. All rights reserved.

Keywords: PEPICO; CH_4^+ ; $\text{C}_2\text{H}_5\text{OH}$; Proton transfer; Electron transfer

1. Introduction

At very low relative collision energies, the cross-section for ion–molecule reactions is determined by the “close collision” cross-section due to the ion-induced dipole interaction [1]. In the region of thermal energies, the capture radius corresponding to this cross-section is considerably larger than the critical distances at which chemical processes and even electron exchange can take place. This situation favours reactions going through a collision complex, a consequence being that, complicated rearrangement and association processes may be possible in addition to simple processes like electron or proton transfer. The probabilities for processes going through a collision

complex are approximately predictable using statistical theories. For increasing relative collision energy, the situation changes in the 1 eV range, because the capture radius for close collisions on the one hand, and the critical distances for chemical reactions on the other, become similar, and both become comparable to the “size” of the combined molecular system. In this situation, it is difficult to estimate the probabilities for the various energetically possible reaction pathways. An experimental study of ion–molecule systems capable of the above indicated different types of reactions in this energy range is therefore of special interest. In addition, knowledge of the dissociation pathways of energised protonated molecules formed in proton transfer processes is of interest in connection with the recently developed method of “proton transfer reaction mass spectrometry (PTR-MS)” [2],

* Corresponding author. E-mail: p.a.zeijlmans@phys.uu.nl

which has turned out to be a very powerful method for the detection of trace gases in the atmosphere [3–5].

We present here results of a study of the ion–molecule system $\text{CH}_4^+/\text{C}_2\text{H}_5\text{OH}$ in the eV collision energy range. In the sense of the introductory outline above, we distinguish the following processes:

- (i) electron exchange: $\text{CH}_4^+ + \text{C}_2\text{H}_5\text{OH} \rightarrow \text{CH}_4 + \text{C}_2\text{H}_5\text{OH}^+$;
- (ii) proton transfer: $\text{CH}_4^+ + \text{C}_2\text{H}_5\text{OH} \rightarrow \text{CH}_3 + \text{C}_2\text{H}_5\text{OHH}^+$;
and the rearrangement processes that can only occur when the collision partners get in close contact, and possibly form a long lived complex, for instance:
- (iii) rearrangement process: $\text{CH}_4^+ + \text{C}_2\text{H}_5\text{OH} \rightarrow \text{C}_3\text{H}_8^+ + \text{H}_2\text{O}$.

Process (i) can occur by transfer of an electron at distances larger than the typical distances necessary for a chemical reaction involving a rearrangement of atoms. Proton transfer (ii) is of course a chemical process, but is distinguished in the present context from the real rearrangement and association processes (iii), because it involves only transfer of the light proton, and does not necessarily require close contact between the colliding molecules. Because of their relative simplicity—and because of the small momentum exchange required between the colliding molecules—we will call processes (i) and (ii) “direct processes.” It should be remembered that, of course, the final channels that are populated in such direct processes, can also be populated by processes going through a complex. On the other hand, the distinction we have made makes sense because if, for some reason, complex formation leading to rearrangement processes does not occur, this will become evident via the observation of solely channels that can be populated in the direct processes. And in addition, a different dependence on the internal energy of the primary ion may be expected for the two types of processes distinguished: while in case of reactions going through a complex, the internal energy of the primary ion is fully available, this is not so for the direct processes, where a large part of it remains in CH_3 , in case of proton transfer (ii), and

in CH_4 in case of charge exchange (i). The influence of the internal energy of CH_4^+ on its reactions with ethanol is studied in our PEPICO experiments.

In case of the present collision system, break-up into three fragments is possible energetically. Corresponding final reaction channels containing three fragments can be populated, in principle, either in two well separated steps, or quasi-simultaneously. In case of the direct reactions, a two-step mechanism appears obvious: a sufficiently large part of the exothermicity of the first direct process is stored in terms of internal energy in the molecular ion formed, and leads to its further dissociation. In case of charge transfer between *atomic* ions and polyatomic molecules, it is well known that the recombination energy of the primary ion is deposited in a (near) resonant way in the quasi-continuum of the energy levels of the polyatomic molecular ion formed in the process [6–8]. In case of charge exchange between a *molecular* ion and a polyatomic molecule, one may expect a similar behaviour, with the modification that the recombination energy is not well defined, leading to a larger region of possible energy transfer to the polyatomic molecular ion.

In the scheme shown in Fig. 1, we show the most relevant reactions our present collision system can undergo. At the left hand side the initial channel is shown, at the right hand side the channels with three fragments, and in the middle the reaction channels with two fragments. The vertical positions in the scheme indicate the relative energy levels of the channels. These energy levels are calculated from thermo-chemical data [9]. The energy values, given in electron volts relative to the initial channel with zero internal energy, are given in brackets for each channel. The arrows are drawn supposing that a two-step mechanism leads to the final channels containing three particles. In the scheme is also indicated the range of energies within which the internal energy (E_{th}) of the initial CH_4^+ ion can be selected using our PEPICO method. The bold Arabic numbers are the ion–mass numbers by which the respective channels can be identified in the measurement.

We point out that the scheme does not contain all possible reaction channels. For clarity, we show only

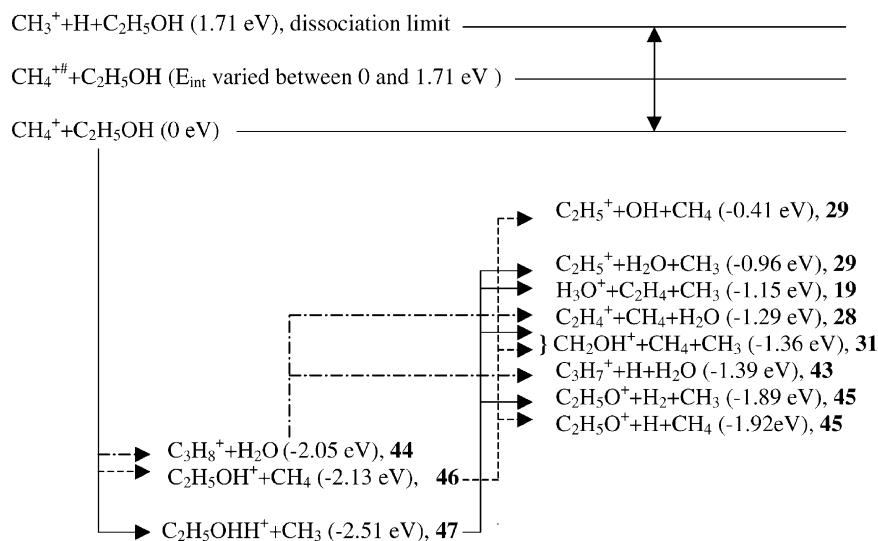


Fig. 1. Scheme of possible reaction channels. Also indicated the minimum channel energies relative to the initial channel with zero internal energy, and the ion masses. The arrows are drawn supposing two-step processes leading to channels with three fragments.

one of the several possible two particle rearrangement channels—the energetically most favourable one leading to formation of C_3H_8^+ and H_2O —and in case of the three particle channels we also show only the energetically most favourable ones. Finally, in case of the further decay of C_3H_8^+ , the possible three particle channel $\{\text{C}_3\text{H}_6^+ + \text{H}_2 + \text{H}_2\text{O} (-1.25 \text{ eV}) \text{ 42}\}$ has been omitted to avoid overcrowding of the scheme.

The experimental results to be presented consist of the relative abundances of the ion fragments formed at different relative kinetic collision energies, and at different internal energies of the initial CH_4^+ . It will be shown that a discussion of the experimental results in terms of the reaction scheme of Fig. 1 leads to a qualitative clarification of the occurring reactions.

2. Experimental

Our PEPICO apparatus has been described earlier in detail [8], we therefore only briefly outline its characteristics. The primary ions—in the present case CH_4^+ —are created by photo-ionisation from neutral molecules effusing from a source at room temperature.

Photons of 21.22 eV of the resonance radiation from a He discharge lamp are used. The primary ions formed are extracted by a voltage pulse (“pulse I”), and guided into a reaction chamber containing the target gas $\text{C}_2\text{H}_5\text{OH}$. In the reaction chamber, the primary ions collide and react with the target gas, whereby the kinetic energy of the primary ions is controlled, and the target gas pressure is kept low enough to guarantee single collision conditions. After a suitable time delay with respect to “pulse I,” the ions residing in the reaction chamber are extracted by a second voltage pulse (“pulse II”) and analysed in a reflectron-type [10] time-of-flight mass spectrometer. The measured mass spectrum in this way consists of unreacted primary ions, and ions created in collisions with CH_4^+ ions of controlled kinetic energy. If “pulse I” is applied immediately after the detection of a photo-electron of a certain selected energy, the mass spectrum contains a component due to primary CH_4^+ ions of selected internal and kinetic energy.

Depending on the photon intensity and the primary gas density, it is possible that not only the primary ion correlated with the detected electron is extracted by “pulse I,” but also one or even several ions for which

the corresponding electron is not detected. These additional ions lead to an *uncorrelated* component of the measured mass spectrum. This *uncorrelated* component can be determined by using a long delay time between the detection of an electron and the sequence of “pulse I” and “pulse II.” To determine the pure *correlated* mass spectrum we chose the following procedure:

- the CH_4 density is adapted in such a way that, at the given photon intensity, the ratio of *correlated* and *uncorrelated* intensities in the detected mass spectrum is about one;
- the $\text{C}_2\text{H}_5\text{OH}$ density is chosen low enough to guarantee single collision conditions for the primary ions;
- the electron spectrometer—with a detection window of 3% of the transmitted energy—is set to a certain transmitted energy;
- per detected electron the extraction sequence of “pulse I” and “pulse II” is applied;

- alternately, the pulse sequence is applied immediately after detection of the photo-electron, and after a long delay time, enough to guarantee that the primary ion belonging to the detected electron does not reside anymore in the region from where the primary ions are extracted by “pulse I”;
- the alternately measured spectra, i.e., the sum of the *correlated* and the *uncorrelated* components, and the purely *uncorrelated* component, respectively, are stored separately and their difference yields the pure *correlated* spectrum.

The *correlated* mass spectrum obtained in this way, consists of accumulated true coincidence pulses at the different flight times corresponding to the different masses. The number of true coincidences per mass region is rather low. In order to obtain a statistical accuracy of the order of 10% for the dominant masses of the spectrum, the required accumulation time is of the order of several days. We therefore restricted our correlated measurements to the four dominant

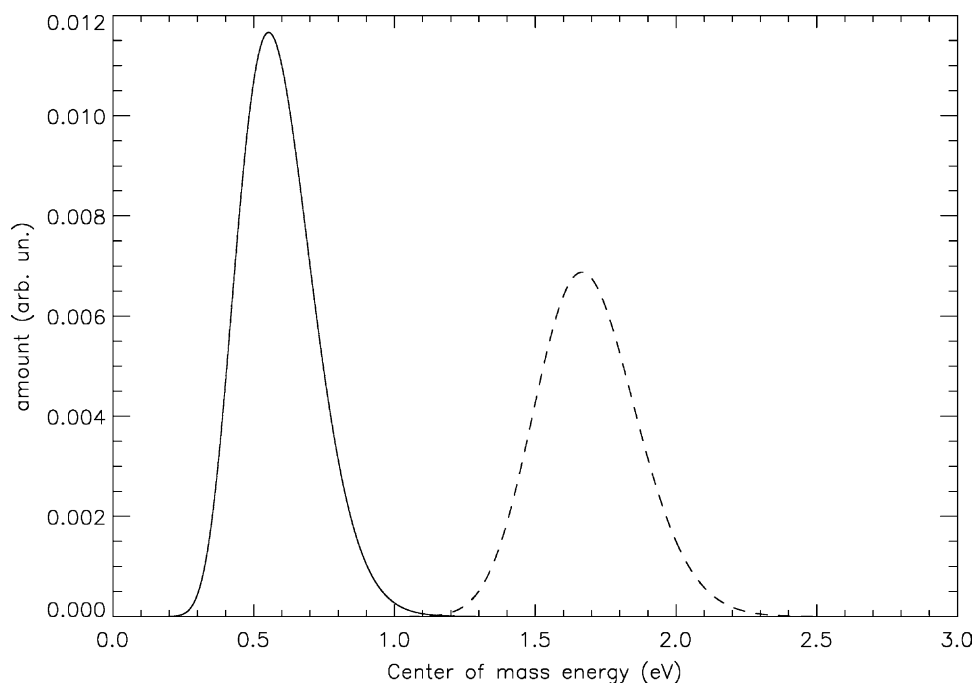


Fig. 2. Relative kinetic energy distributions resulting from a given acceleration voltage of the CH_4^+ ion. The two cases of acceleration voltages of 1 and 2.5 eV are shown.

ion masses. Since our electronic routing system restricts us to the simultaneous measurement in at most four different mass channels, whereby one of them has to be the parent ion mass channel for calibration purposes, we combined in an actual run either the higher masses 46 and 45 in one mass window, and intensities of the lower masses 31 and 29 in separate mass windows, or we combined the lower masses and measured the higher masses separately. We obtained the corresponding *correlated* spectra for five different kinetic energies, and for each kinetic energy for different internal energies.

The relative kinetic energy distribution corresponding to a well-defined acceleration of the primary ion, is rather broad due to both, the thermal velocity distribution of the CH_4 molecules prior to ionisation, and the thermal velocity distribution of the target. The situation is exemplified in Fig. 2, where we show two centre-of-mass energy distributions arising for primary CH_4^+ ions moving initially towards the

reaction chamber with a velocity corresponding to 40 meV kinetic energy. One distribution is calculated for the case of an acceleration voltage of 1 eV, and one for an acceleration voltage of 2.5 eV. The energy of the maximum of such a distribution will in the following be called “the relative kinetic energy.”

A quick overview of ion spectra not correlated with a certain photo-electron energy can be obtained by triggering “pulse I” electronically at a certain rate, and choose an optimised delay time for “pulse II.” An example of such a non-coincident spectrum is shown in Fig. 3. We see four significant peaks at the masses 46, 45, 31, and 29, and smaller peaks at masses 47, 27, and 19. The intensities at lower masses are not shown since this part of the spectrum is dominated by contributions from primary ion masses (with much higher intensities). The mass resolution of the reflectron itself is about 200, however, the resolution for the product ions formed from primary ions entering the reaction chamber is less, due to the time width of the

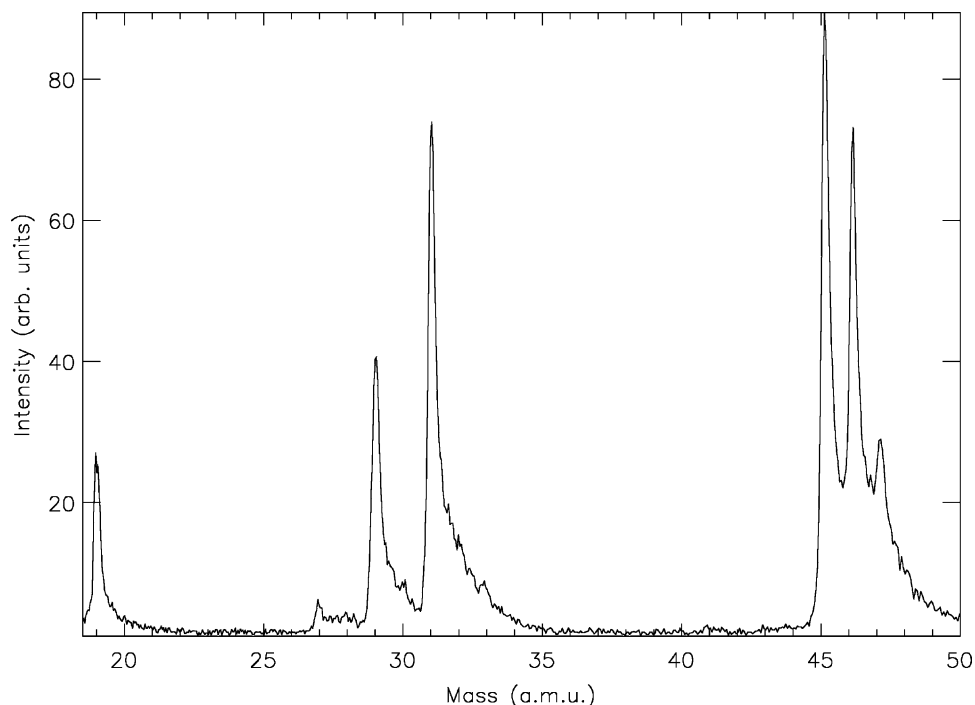


Fig. 3. Non-coincident ion mass spectrum resulting from collisions of CH_4^+ with $\text{C}_2\text{H}_5\text{OH}$.

primary ion pulse. A tail extending towards higher masses is caused by product ions being formed at later times from the primary ions.

Correlated relative ion intensities are obtained for the masses 46, 45, 31, and 29 for five different kinetic energies, and for several internal energies.

3. Results and discussion

To facilitate the following discussion we indicate in the first two columns of Table 1, the correspondence between mass number and fragment ion.

A very direct qualitative clarification of the reactions occurring in the $\text{CH}_4^+/\text{C}_2\text{H}_5\text{OH}$ system follows already from the non-coincident spectrum shown in Fig. 3. The ion masses 44 and 28, which, according to the scheme in Fig. 1, are indicative of rearrangement and association reactions, are not present. The same is true for other masses that can only be formed in rearrangement processes. It is therefore clear that only the direct reactions occur. Further, since only proton transfer can lead to formation of the ion of mass 47, and only charge exchange can lead to the formation of the ion of mass 46, the contribution of both these direct processes is evident. While the fragments of masses 45 and 31 can be formed via both direct processes, as indicated in the scheme in Fig. 1, the fragment of mass 29 is probably solely due to proton transfer followed

by dissociation. We conclude this from the fact that the break down pattern of the energised ethanol molecular ion [11] does not show a significant contribution of the C_2H_5^+ fragment in the internal energy range relevant for the present case ($E_{\text{int}} < 4 \text{ eV}$). We checked the absence of C_2H_5^+ in the mass spectrum of ethanol photo-ionised by 21.22 eV photons from our source, and found indeed less than 1% mass 29 fragment ions in the spectrum containing the masses 46, 45, and 31.

We can compare our results regarding the decay of excited ethanol and protonated ethanol ions formed in charge exchange and proton transfer reactions with CH_4^+ , with results obtained by Kubista et al. [12], who studied the decay of the same molecular ions after excitation by collisions with a surface. These authors measure, for the case of excited ethanol molecular ions, significant fragment ion intensities at the masses 46, 45, 31, and 28. Making use of the known break down pattern of ethanol ions [11], they deduce a broad internal energy distribution that peaks around 2 eV, and extends from zero to almost 4 eV. Interestingly, we do not observe any intensity at mass 28, as emphasised above. Based on the break down pattern of the ethanol ion [11], this difference could be explained by assuming that the internal energy distribution of the ethanol ion formed by electron exchange with CH_4^+ is much narrower than in case of excitation in surface scattering: if the internal energy distribution would peak around the resonance energy,

Table 1
The first two columns give the ion masses and the corresponding ion fragment

Mass (amu)	Ion fragment	Relative abundance (%)	Reaction (see Fig. 1)
19	H_3O^+	≈ 9	Proton transfer
27	C_2H_3^+	≈ 1	Proton transfer
28	C_2H_4^+	Not observed	Rearrangement
29	C_2H_5^+	15 ± 2	Proton transfer
31	CH_2OH^+	35 ± 5	Proton transfer and electron transfer
44	C_3H_8^+	Not observed	Rearrangement
45	$\text{C}_2\text{H}_5\text{O}^+$	22 ± 4	Proton transfer and electron transfer
46	$\text{C}_2\text{H}_5\text{OH}^+$	22 ± 4	Electron transfer
47	$\text{C}_2\text{H}_5\text{OHH}^+$	≈ 5	Proton transfer

In the third column, the relative abundances of the fragments formed in reactions of CH_4^+ with $\text{C}_2\text{H}_5\text{OH}$ are given. The numbers with the (\approx) sign are taken from the non-coincident spectrum, and the others are obtained by averaging the relative intensities of the *correlated* mass spectra. In the last column, the respective reaction paths are indicated.

i.e., the difference between the ionisation energies of CH_4 and ethanol, 2.13 eV—and if it would not extend towards low energies beyond ca. 1.8 eV, the missing intensity at mass 28 would be consistent with the break down pattern. For the case of protonated ethanol excited in surface collisions [12], the mass spectrum shows significant intensities at the masses 47, 29, 27, and 19. This is in qualitative agreement with the present results. The absence of mass 31 in the spectrum of [12] suggests that, probably, in the spectrum due to collisions of CH_4^+ with ethanol, fragments of mass 31 are solely due to charge transfer followed by decay of the excited ethanol ion. Since, according to the break down pattern of the ethanol ion, an internal energy higher than about 2 eV is necessary for this decay to occur with appreciable probability, this is additional support for a narrow internal energy distribution peaking around 2.13 eV, as invoked above to explain the absence of ion fragments of mass 28.

The result of a typical measurement of the *corrected* relative ion intensities is shown in Fig. 4. The intensities of the ion masses 45, 46, and of the sum

of the masses 31 and 29, are given in percent of the intensity of the parent ion mass 16, as a function of the internal energy. The ratio of the ion intensities of the masses 31 and 29 (see Table 1) is independent of the internal energy within statistical error. The chosen relative kinetic energy was 1 eV. We notice that the variations of the ion intensities lie inside the statistical error given by the error bars. At the first sight, this is a surprising result in view of the fact that the internal energy range subtended is of the order of the exothermicity of the reactions observed. On the other hand, the result supports our first qualitative conclusion drawn from the non-coincident spectrum discussed above, namely, that only proton transfer and charge exchange processes occur, and no reactions involving a complex. While for reactions involving a complex, the whole internal energy of the primary ion is available and determines the fragmentation of the complex, this is not the case for the direct processes, where the internal energy of the molecular ions formed—in our case the ions $\text{C}_2\text{H}_5\text{OH}^+$, and $\text{C}_2\text{H}_5\text{OHH}^+$ —is in first order independent of the internal vibration–rotational

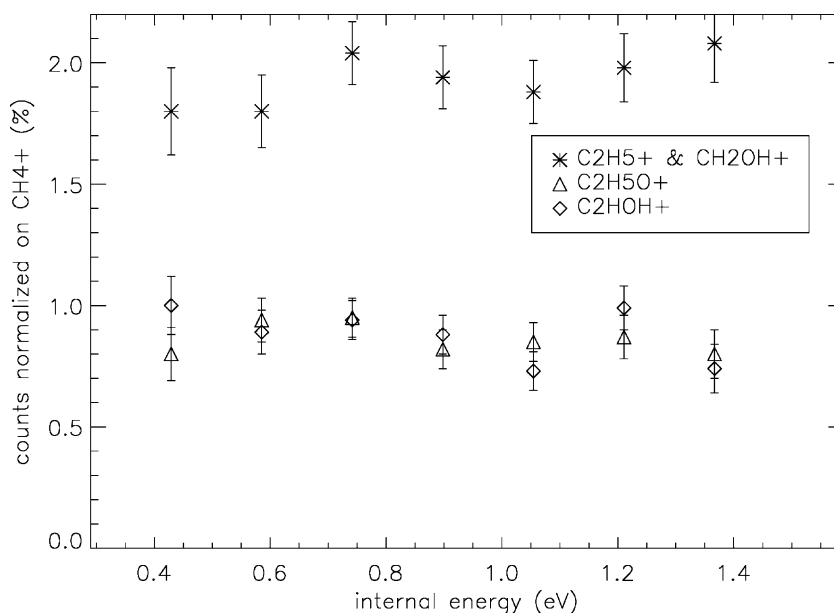


Fig. 4. Relative ion intensities, in percent of the intensity of the primary CH_4^+ ion, as a function of the internal vibration–rotational energy of CH_4^+ , and for a relative kinetic energy of 1 eV. Three mass channels are distinguished: the channel containing the masses 31 and 29, the channel containing the mass 45, and the channel containing the mass 46.

energy of the primary ion. Measurements at different kinetic energies and for the two combinations of ion masses mentioned above, gave similar results: no significant variation of the ion intensities as a function of internal energy of the primary ion.

The measurements of *correlated* mass spectra for a fixed internal energy and different kinetic energies in the range from 0.2 to 5.6 eV also showed no significant variation of the relative ion intensities. This result is consistent with the dominance of direct reactions, and suggests that these direct reactions occur preferably in “distant collisions” around fixed transition distances where either an electron is transferred from the target molecule to the primary ion, or a proton is transferred from the primary ion to the target molecule.

In the absence of significant variations of the mass spectra as a function of both, the internal energy of the primary ion, and the relative collision energy, we are able to determine the relative ion intensities by averaging the *correlated* mass spectra. The result is given in column 3 of Table 1. The intensities are very similar to the ones observed in the non-coincidence spectrum, however, some possibilities for systematic errors due

to a spurious admixture of the target gas to CH_4 density in the ionisation volume are excluded. In the table we also give a value for masses 47, 27 and 19. These values are taken from the non-coincident spectrum.

4. Summary

Our experimental study of the ion–molecule system $\text{CH}_4^+/\text{C}_2\text{H}_5\text{OH}$ by the PEPICO method in the range of 0–1.7 eV of internal energies of the CH_4^+ ion, and 0.2–5.6 eV of relative collision energies, have shown that only the direct processes of electron and proton transfer occur, and that rearrangement and association processes play a negligible role in the whole region of varied internal and kinetic energies. The molecular ions formed in these direct reactions, $\text{C}_2\text{H}_5\text{OH}^+$, and $\text{C}_2\text{H}_5\text{OHH}^+$, respectively, are found to partly further fragment, leading to final channels containing three fragments. The relative abundance of ion fragments formed, is found to be approximately constant in the whole range of varied internal and kinetic energies. This indicates that the reactions are due to transitions

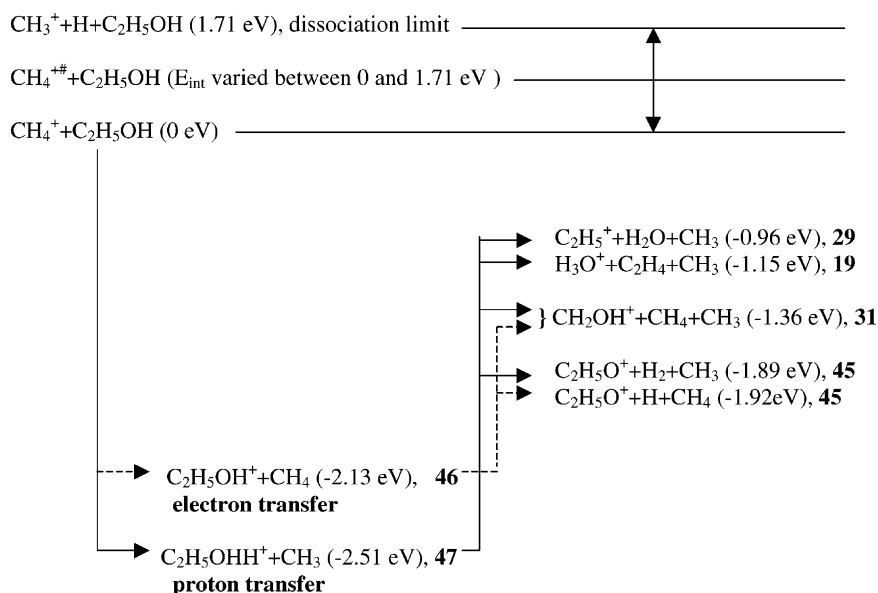


Fig. 5. Scheme of the reactions found to occur in collisions of CH_4^+ with $\text{C}_2\text{H}_5\text{OH}$. The reactions proceed in two steps, whereby the first step is either a proton transfer or an electron transfer. Both these direct processes occur with comparable probability. No indication of rearrangement processes is found.

involving electron or proton transfer at relatively fixed distances, whereby the internal energy of the molecular ion formed is nearly independent of both, the internal energy of the primary ion and the relative collision energy. These results can be summarised in the reaction scheme shown in Fig. 5.

References

- [1] G. Gioumousis, D.P. Stevenson, *J. Chem. Phys.* 29 (1958) 294.
- [2] W. Lindinger, A. Hansel, A. Jordan, *Int. J. Mass Spectrom. Ion Process.* 173 (1998) 191.
- [3] J. Williams, U. Pöschl, P. Crutzen, A. Hansel, R. Holzinger, C. Warneke, W. Lindinger, J. Lelieveld, *J. Atm. Chem.* 38 (2000) 133.
- [4] U. Pöschl, J. Williams, P. Hoor, H. Fischer, P. Crutzen, C. Warneke, R. Holzinger, A. Hansel, A. Jordan, W. Lindinger, H. Scheeren, J. Lelieveld, *J. Atm. Chem.* 38 (2000) 115.
- [5] C. Warneke, R. Holzinger, A. Hansel, W. Lindinger, J. Williams, U. Pöschl, P. Crutzen, *J. Atm. Chem.* 38 (2000) 167.
- [6] Z. Herman, B. Friedrich, *J. Chem. Phys.* 102 (1995) 7017.
- [7] C. Praxmarer, A. Hansel, W. Lindinger, *J. Chem. Phys.* 109 (1998) 4246.
- [8] A.Y. Kok, P.A. Zeijlmans van Emmichoven, A. Niehaus, *Chem. Phys.* 258 (2000) 47.
- [9] NIST Chemistry Webbook, National Institute of Standards and Technology, <http://webbook.nist.gov>, 2000.
- [10] B.A. Mamyrin, V.I. Karataev, D.V. Shmikk, V.A. Zagulin, *Sov. Phys. JETP* 37 (1973).
- [11] L. Friedman, F.A. Long, M. Wolfsberg, *J. Chem. Phys.* 32 (1960) 149.
- [12] J. Kubista, Z. Dolejssek, Z. Herman, *Eur. Mass Spectrom.* 4 (1998) 311.